smart cities

MDPI

Article

Assaying Traffic Settings with Connected and Automated Mobility Channeled into Road Intersection Design

Maria Luisa Tumminello [1,*], Nazanin Zare [1], Elżbieta Macioszek [2,*] and Anna Granà [1]

[1] Department of Engineering, University of Palermo, 90133 Palermo, Italy; nazanin.zare@unipa.it (N.Z.); anna.grana@unipa.it (A.G.)
[2] Department of Transport Systms, Traffic Engineering and Logistics, Faculty of Transport and Aviation Engineering, Silesian University of Technology, 44-100 Katowice, Poland
* Correspondence: marialuisa.tumminello01@unipa.it (M.L.T.); elzbieta.macioszek@polsl.pl (E.M.)

Highlights

What are the main findings?

- Integrating road intersection geometric design with smart vehicle technologies enhances the benefits of well-designed road infrastructure, optimizing traffic efficiency as the prevalence of smart vehicles continues to rise.
- Traffic settings involving connected and automated vehicles (CAVs) can inform the design of road intersections within the context of smart cities, using microsimulation to analyze performance in mixed urban traffic environments.

What is the implication of the main finding?

- Support the development of expertise in the comparative analysis of the performance of alternative intersection designs that incorporate smart vehicle technologies.
- The microsimulation-driven framework underlines the importance of effective calibration to promote the development of evaluation methodologies for intersection designs and smart mobility integration in city planning.

Abstract: This paper presents a microsimulation-driven framework to analyze the performance of connected and automated vehicles (CAVs) alongside vehicles with human drivers (VHDs), channeled towards assessing project alternatives in road intersection design. The transition to fully automated mobility is driving the development of new intersection geometries and traffic configurations, influenced by increasing market entry rates (MERs) for CAVs (CAV-MERs), which were analyzed in a microsimulation environment. A suburban signalized intersection from the Polish road network was selected as a representative case study. Two alternative design hypotheses regarding the intersection's geometric configurations were proposed. The Aimsun micro-simulator was used to hone the driving model parameters by calibrating the simulated data with reference capacity functions (RCFs) based on CAV factors derived from the Highway Capacity Manual 2022. Cross-referencing the conceptualized geometric design solutions, including a two-lane roundabout and an innovative knee-turbo roundabout, allowed the experimental results to demonstrate that CAV operation is influenced by the intersection layout and CAV-MERs. The research provides an overview of potential future traffic settings featuring CAVs and VHDs operating within various intersection designs. Additionally, the findings can support project proposals for the geometric and functional design of intersections by highlighting the potential benefits expected from smart driving.

Academic Editor: Pierluigi Siano

Received: 2 April 2025
Revised: 16 May 2025
Accepted: 21 May 2025
Published: 25 May 2025

Citation: Tumminello, M.L.; Zare, N.; Macioszek, E.; Granà, A. Assaying Traffic Settings with Connected and Automated Mobility Channeled into Road Intersection Design. *Smart Cities* **2025**, *8*, 86. https://doi.org/10.3390/smartcities8030086

Keywords: sustainable road design; roundabouts; signalized intersections; knee-turbo roundabout; smart mobility; connected and automated vehicles; traffic microsimulation

1. Introduction

As urban populations grow, the demand for smart mobility is increasing, creating a need for reliable, efficient, and environmentally friendly transportation systems. Road engineering professionals face the challenge of developing innovative solutions that can accommodate rising mobility demands while integrating advanced technologies into the design of smart roads [1]. Recent advancements in Intelligent Transport Systems (ITS), particularly those involving connected and automated vehicles (CAVs), offer new opportunities to enhance road performance and promote sustainability from both research and policy perspectives [2]. CAVs use communication technologies to exchange information with each other, road infrastructure, and other entities for improved traffic management [3]. As automation levels increase, these advancements decrease driver workload and human unpredictability, resulting in a more efficient driving experience for all road users [4]. The deployment of CAVs is expected to provide numerous benefits, including fewer crashes, increased road capacity, optimized mobility, reduced emissions, improved road quality, and enhanced overall well-being for citizens [5,6]. However, several challenges related to the practical implementation and impact of CAVs remain unresolved, as high levels of automation are not yet commercially widespread. As CAVs gradually replace vehicles with human drivers (VHDs), their interactions become increasingly important, particularly at intersections where different traffic streams converge [6,7]. CAVs are equipped with communication and control devices like cooperative adaptive cruise control (CACC), which optimizes traffic efficiency by adjusting speed and distance relative to the preceding vehicle [8]. Although low CAV penetration rates present challenges, CAV platoons can travel closely to minimize delays safely, but CAVs may drive cautiously when interacting with VHDs lacking communication technology [9].

Interactions between CAVs and VHDs can vary significantly, particularly at unsignalized intersections, where the cautious and hesitant driving behavior of human-operated vehicles can complicate yield negotiations [10]. Conversely, signalized intersections facilitate decision-making for gap acceptance with clear traffic signals [1,7]. Although roundabouts are typically less expensive to install and maintain than signalized intersections, CAVs face challenges when navigating curved trajectories in multilane scenarios, especially regarding gap acceptance and lane-changing [11–13]. The transition from two-lane to turbo roundabouts introduces lane dividers or curbs to separate traffic streams, requiring the pre-selection of entry lanes and thus facilitating navigation for vehicles [14,15].

Research on CAVs increasingly utilizes micro-simulation models to assess performance in mixed traffic environments [2,16,17]. These simulations aim to analyze the dynamic CAV–infrastructure interactions and entry negotiation processes between CAVs or between a CAV and a VHD at intersections, while evaluating the effectiveness of algorithms in real-world scenarios [18,19]. Findings indicate that smart vehicles outperform VHDs in capacity and saturation headways due to their connectivity and automation, even at varying levels of communication [20,21]. Ongoing research also investigates trajectory design for CAVs and VHDs to improve operations at signalized intersections, employing deep reinforcement learning for optimal efficiency [22,23]. The optimization of CAV trajectories at roundabouts also shows significant performance improvements as penetration rates rise, leading to reduced travel times [24]. To establish effective navigation rules for roundabouts, optimal vehicle path management is essential; however, employing machine learning methods or

more advanced algorithms can be beneficial but they often incur significant computational costs and prolonged processing times due to their iterative nature. Furthermore, while micro-simulation results offer valuable insights, they are typically specific to individual studies, necessitating diverse evaluations of case scenarios for broader generalizability across different contexts [13]. The study in [25] similarly highlights variability in CAV behaviors and the importance of mixed traffic with VHDs. Although focused on an expert system for a single-lane roundabout, it emphasizes broader applicability across intersection types, addressing the need for adaptable, inclusive traffic management solutions for emerging CAV technologies.

In the context of smart cities, although advancements in CAV technology and their testing on road infrastructures can inform the design of smart intersections and roundabouts [1,2,25], the broader challenges of managing and optimizing CAV operations at intersections remain unresolved and require further research [25,26]. Specifically, there is a gap in the literature regarding published studies that compare various intersection geometric design proposals in terms of CAV performance in mixed traffic environments. In this broader context of the interaction between CAVs and road infrastructure, this paper aims to address that gap by evaluating different intersection design options and analyzing their impact on the operational efficiency of CAVs. In this perspective, it aligns with the evolving needs of professionals in the field of road design.

Based on the above, a microsimulation-driven framework for analyzing the performance of CAVs alongside VHDs is proposed. The aim of this paper is to investigate how traffic scenarios involving connected and automated mobility can be channeled into the design of road intersections, thereby promoting the sustainable integration of smart vehicles into current and future road infrastructure. The primary objective is to explore the role of microsimulation, particularly using Aimsun (Version 20) [17], to compare the performance of CAVs in mixed traffic environments and various intersection layouts, focusing on the following key questions:

- To what extent can the calibration process of Aimsun's parameters replicate simulated data that align with the reference capacity functions (RCFs) for a given road entity?
- What is the impact of the geometric and functional design of intersections, along with traffic control modes, on the expected operational performance of CAVs as their market entry rates (MERs) vary?
- Is it feasible to develop a performance criterion that enables the comparison of alternative geometric designs of intersections based on the analogy of entry mechanisms?

A suburban, four-legged signalized intersection in a Polish city was selected as a case study. Various traffic scenarios with different MERs for CAVs (CAV-MERs) were modeled in Aimsun, including two proposed roundabout solutions: a two-lane roundabout and a knee-turbo counterpart, which served as testbeds in the validation-driven approach based on the analogy in entry mechanisms. Inspired by the turbo roundabout design detailed in [14,27], the knee-turbo geometry was developed as an alternative layout designed to accommodate travel demands within the examined intersection area and its surrounding built environment. Traffic and geometric data were configured in Aimsun to match the conceptual scenarios, and sensitive driving model parameters were adjusted to align the simulated data with the RCFs, considering the increasing CAV-MERs and correction factors sourced from [13].

Cross-referencing various geometric design solutions for the signalized intersection, including the two-lane roundabout and the knee-turbo scheme, revealed that CAV operations are affected by intersection layouts and the CAV-MERs. In this perspective, the study proposes a methodological framework to evaluate future intersection designs by integrating CAV technology with road engineering. Additionally, the framework can

serve as a complementary tool in geometric and functional design, facilitating the assessment of how modifications in intersection schemes influence CAV performance. Thus, the paper offers a helpful methodology for assessments throughout the design process, aiding decision-making on alternative project proposals that leverage the benefits of smart driving—an approach commonly used in feasibility studies before detailed project development. However, additional case studies of intersections with various control types are needed to ensure the broader applicability of the proposed method across different road entities and urban environments and to enable the effective generalization of the results. In addition to its scientific contribution in assessing future traffic scenarios with CAVs and VHDs at intersections, the paper fosters a culture of ITS and promotes smart mobility, aiming to raise awareness among citizens and road users about the advantages of a safer, more appealing, and less polluted road environment.

The paper is structured as follows: It begins with an introduction, followed by the research materials and methods in Section 2, outlining the case study description, design alternatives, and Aimsun network modeling. Section 3 presents the results, while Section 4 discusses them. Finally, Section 5 concludes the paper.

2. Materials and Methods

The microsimulation-driven framework proposed in this paper for analyzing the performance of CAVs alongside VHDs at various intersection designs follows the steps shown in Figure 1.

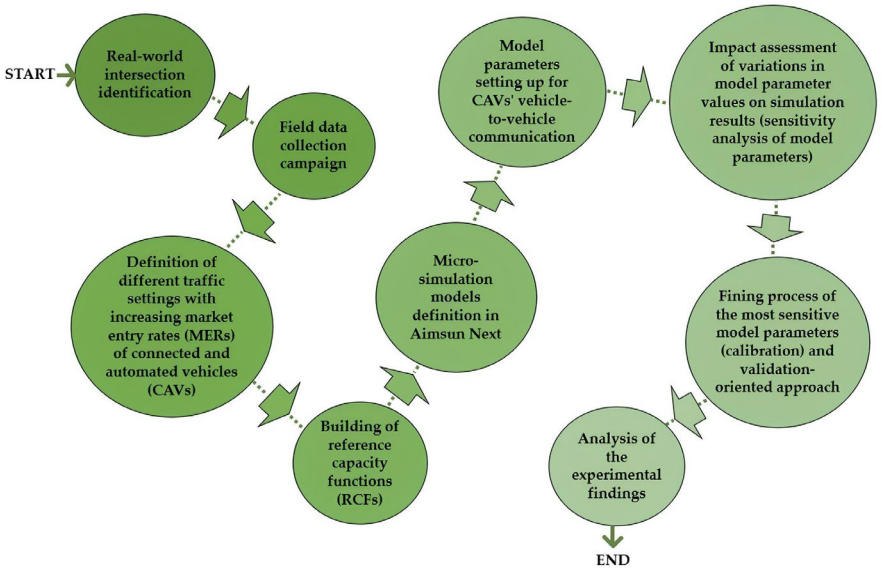

Figure 1. Bubble chart to map the research methodology.

The initial phase of the study focused on selecting a representative signalized intersection within a suburban urban setting, taking into account its spatial layout, traffic patterns, and operational features. Field data collection was carried out to gather detailed information on traffic flows, vehicle types, and signal control mechanisms. Using the existing intersection design as a foundation, a new proposal was developed to replace the signalized intersection with a two-lane roundabout, with the goal of converting it into a turbo roundabout. This approach aims to improve traffic throughput, safety, and efficiency by optimizing the intersection's geometric and operational characteristics.

The next step involved establishing traffic settings with CAV-MERs, varying from 0% to 100% in 20% intervals. Subsequently, for each intersection, capacity functions were developed corresponding to these CAV-MER levels. These functions incorporated correction

factors specific to CAVs from [13], reflecting their impact on intersection performance as their MER increases. This analysis helps in understanding how different CAV-MERs can influence intersection capacity and operational efficiency.

In Aimsun, vehicle-to-vehicle (V2V) communication for CAV fleets was implemented to simulate traffic conditions for the proposed intersection layouts. Subsequently, a sensitivity analysis of the model parameters was conducted before calibrating them. The calibration process involved comparing the simulated output data—based on the most sensitive model parameters—with the RCFs at roundabouts. The calibration accuracy for the signalized intersection model was assessed by varying the green time values within the traffic light cycle at different CAV-MER levels.

The knee-turbo roundabout served as a counterpart for validating the simulated two-lane roundabout model, based on the analogy in their entry mechanisms by entry approach. In the subject approach selected for the analysis, the left lane experienced conflicts from two circulating traffic flows, while the right lane encountered a single circulating flow. Thus, the right lane of the two-lane roundabout was considered a de facto right-turn lane, conflicting with the one-lane circulatory roadway, to facilitate a comparative operational analysis between the two conceptualized roundabouts. This validation-driven approach offered an additional tool for assessing the calibration effectiveness of the intersections under study. Ultimately, selected key performance metrics were employed to evaluate and compare CAV performance across the different intersection layouts and traffic settings.

2.1. Case Study Description

To analyze the performance of a mixed fleet of CAVs and VHDs at various intersection types and their associated traffic regulation modes, we selected a suburban, isolated four-legged signalized intersection within the road network of Opole City, Poland (50°39′17″ N; 17°57′16″ E), which was well-suited to effectively facilitate the development of diverse design proposals. The selected signalized intersection consists of a main road, "Jerzego i Ryszarda Kowalczyków", which has two entry lanes, each 3.25 m wide, and one exit lane measuring 3.50 m in width. The main road directs traffic towards the center of Opole City in the north-west direction, while in the south-eastern direction it transitions into the DK 94 highway, which leads to the hamlet of Strzelce Opolskie. The minor road consists of "Mieszka I" street, extending in the north-easterly direction, featuring two entry lanes, each 3.25 m wide, and one exit lane measuring 3.50 m wide. In the south-westerly direction, "Jagiellonów" street includes three entry lanes that are 3.25 m wide and one exit lane that is 3.50 m wide. The signalized intersection comprises four approaches, each featuring one shared right-turn and through lane (R&T) plus an exclusive left-turn lane (L), except for the south-west (S-W) approach, which has three entry lanes for each movement. Figure 2 illustrates key details of the intersection under study, while Figure 3 shows the main results of the field data collection that took place during morning and afternoon peak hours in September 2024.

Data on the signal timing plan, traffic movements, and vehicular composition were recorded using a camera positioned along the west-north (W-N) approach. Post-processing of this field data revealed an average traffic volume of 2263 vehicles per hour, primarily consisting of cars, with a small percentage of heavy vehicles, as shown in Figure 3a. Additionally, minimal percentages of pedestrians and cyclists were observed, likely due to the suburban context of the intersection's location. The traffic light timing was analyzed without including pedestrians and cyclists, but in urban areas with higher pedestrian volumes, their phase would be incorporated into and extend the cycle duration.

Due to the low presence of pedestrians and cyclists in the suburban setting, these users were excluded from the subsequent analysis of the two-lane roundabout and its

knee-turbo counterpart. Typically, pedestrians and bicyclists navigate roundabouts via separated shared-use paths, with crossings set back from the circulatory roadway and protected by splitter islands for safe two-stage crossing [12,28]. Bikers should feel as safe as or safer than approaching drivers, but their safety must not compromise pedestrian safety. Multi-lane roundabouts often incorporate active traffic control devices, requiring pedestrians to activate signals [12]. Pedestrian accommodations in turbo roundabouts are like those found in modern roundabouts [27].

(**a**) (**b**)

Figure 2. The signalized intersection under study: (**a**) geometric scheme sketch; (**b**) photo of the E-S entry approach. Note: the acronyms are provided in the legend.

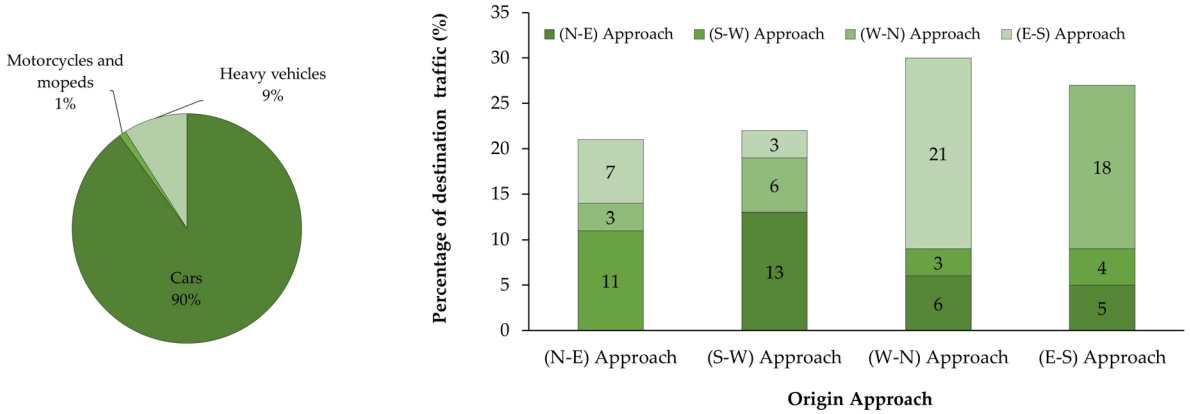

(**a**) (**b**)

Figure 3. Traffic features: (**a**) pie graph on the vehicular composition; (**b**) histogram chart of origin–destination traffic by approach.

The distribution of maneuvers among various approaches at the signalized intersection under study is as follows: 39% of the total traffic on the main road engaged in crossing maneuvers, while 10% of users made left turns and 8% made right turns. Figure 3b illustrates the percentages of destination traffic for each origin approach. Crossing traffic on the minor road constituted 24%, which included 11% of traffic flowing from the north-eastern (N-E) origin to the south-western (S-W) destination, while the remaining 13% pertained to the opposite direction. Additionally, the percentage of left turns from the S-W approach to the main road was approximately 6%, with right turns at around 3%. Conversely, from the N-E approach to the main road, left turns were about 7%, while right turns were around 3%.

The traffic light operated on a four-phase timing plan in the fixed mode, with a total cycle length of 120 s, as illustrated in Figure 4.

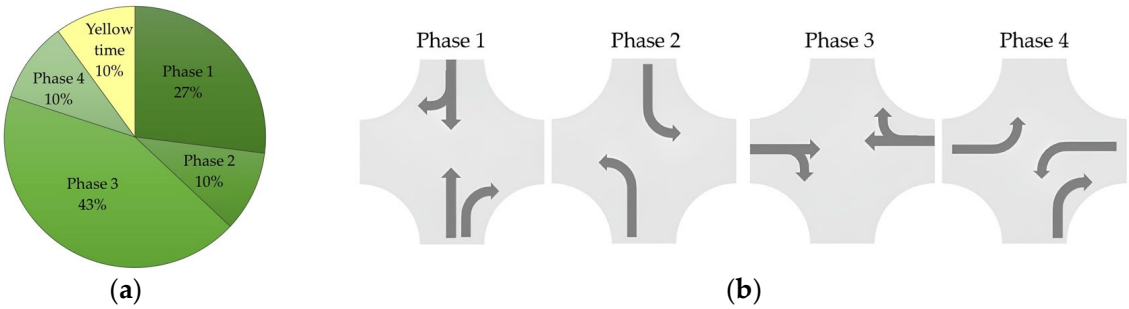

Figure 4. The timing plan: (**a**) pie graph on the green time percentage for each phase of the traffic signal; (**b**) the four-phase timing plan diagram with the allowable movements.

Figure 4a displays the green time percentage for each phase, while Figure 4b shows the four-phase timing plan diagram with the allowable movements during each phase at the signalized intersection. In Phase 1, right turns and through traffic on the north-eastern (N-E) and south-western (S-W) minor roads receive a green time of 27% of the total cycle length. During Phase 2, left-turning traffic from the minor road to the main road is allocated a green time of 10% of the cycle. Phase 3 grants 43% of the cycle to right turns and through movements on the main road. Finally, Phase 4 permits left-turning traffic from the west-north (W-N) and east-south (E-S) main roads, as well as right-turning traffic from the south-west (S-W) minor road, to operate for 10% of the cycle.

Consistent with [13], lane groups were established at the signalized intersection: exclusive left turns were classified as an individual lane group, while right turns and through movements shared a single lane group. This arrangement facilitated the conceptualization and formulation of various design proposals, including the potential for roundabouts.

Considering the available space for a circular layout, the suburban context of the installation, and the traffic composition, an initial design for a two-lane roundabout was developed to transition the existing signalized intersection into a knee-turbo roundabout [14,27]. Figure 5 presents the geometric sketches of the designed two-lane roundabout (see Figure 5a) and the knee-turbo roundabout (see Figure 5b). Additionally, Figure 5c,d illustrates the conflict points for the two-lane roundabout and the knee-turbo roundabout, respectively. Changes in conflict points and vehicle path designs can aid in the comparative analysis of the roundabouts, offering better insights into how different geometric layouts influence CAV performance.

The designed four-legged roundabout featured two entry lanes and one exit lane for each approach except for the S-W approach, as shown in Figure 5a. It included a non-traversable central island and an outer diameter of 26 m, along with two circulatory lanes, each measuring 3.75 m wide. The geometric design also integrated raised splitter islands and deflection angles exceeding 45 degrees.

A knee-turbo roundabout was subsequently conceptualized and designed (see Figure 5b). Inspired by the turbo roundabout design detailed in [14,27], this geometry was developed as an alternative tailored to meet the travel demands within the intersection area and its surrounding built environment. The knee-turbo roundabout is a specialized variation of the basic turbo roundabout, distinguished by its distinctive geometric features [14,27].

Unlike the basic version, the knee-turbo features a more pronounced angular shape—resembling a knee—often involving tighter curves and strategic lane arrangements to enhance the integration of multiple traffic streams. It typically incorporates dedicated lanes for different movement types, such as turning and straight-through flows, which further reduce weaving conflicts common in modern roundabouts [12,14,27]. One key advantage of the knee-turbo design is its improved ability to effectively slow vehicles

before they enter the circulating roadway, thereby reducing crash risks and enhancing adaptability in complex traffic environments, all while maintaining efficient vehicle circulation. Although it provides similar traffic throughput to the basic turbo roundabout, the knee-turbo roundabout offers greater flexibility in configuring entry approaches, allowing for various lane combinations in the entry, exit, and circulatory roadway along the opposing approaches [14,27]. While safety parameters for turbo roundabouts are generally well established—particularly when comparing the basic turbo to two-lane roundabouts [12,14,27]—considering these characteristics during the design process is essential to mitigate the risks of over- or under-dimensioning in the evaluated schemes.

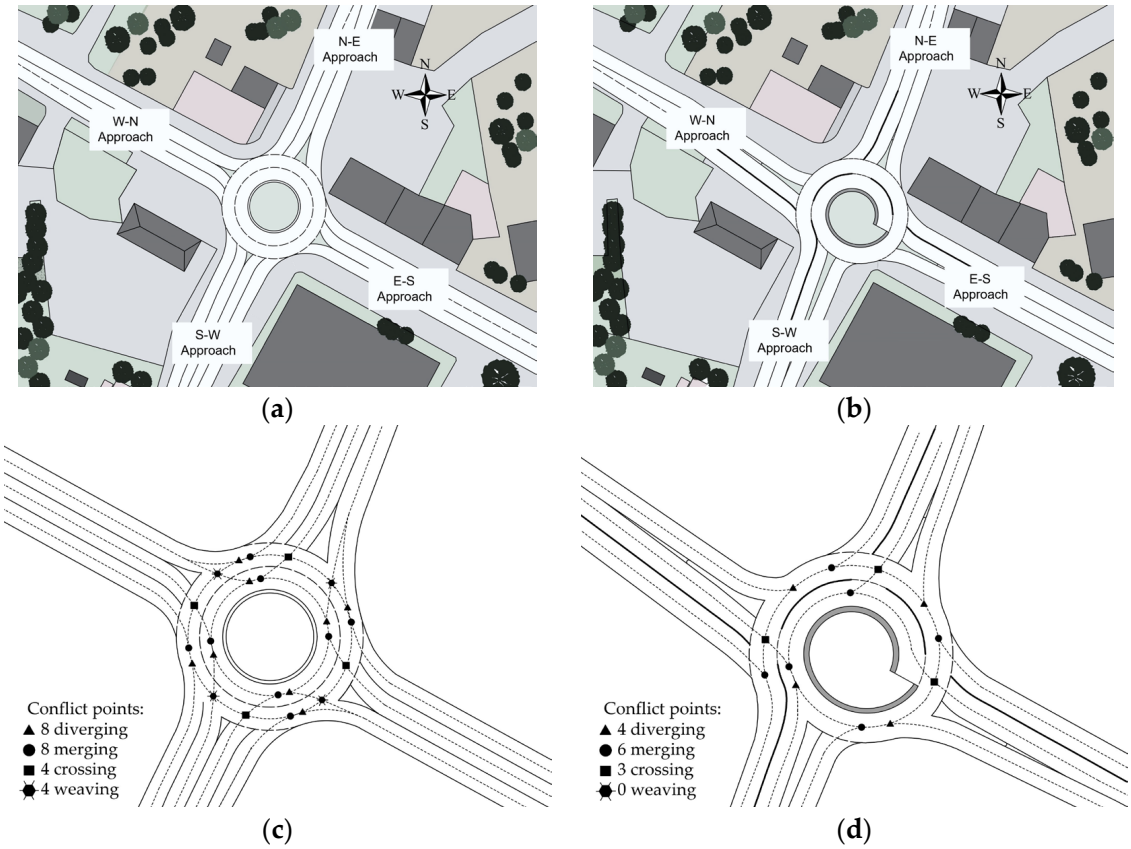

Figure 5. Geometric sketch of (**a**) the designed two-lane roundabout; (**b**) the knee-turbo roundabout; (**c**) the conflict points at the two-lane roundabout; (**d**) the conflict points at the knee-turbo roundabout. Note: N-E stands for north-east, E-S stands for east-south, S-W stands for south-west, and W-N stands for west-north. Note: The acronyms are provided in the legend.

The footprint of the knee-turbo roundabout was adapted to accommodate the two-lane layout, optimizing the available installation space (see Figure 5b). The main road features two entry lanes and one exit lane in the west-north (W-N) and east-south (E-S) directions. The minor road includes two entry lanes and one exit lane in the north-east (N-E) direction, while in the south-west (S-W) direction, it has one entry lane and two exit lanes. Each entry lane is 3.75 m wide, each exit lane is 3.50 m wide, and each circulating lane measures 4.00 m in width. The splitter islands comply with Polish guidelines, ensuring effective traffic management and safety within the roundabout design [29].

The knee-turbo roundabout is introduced as a new conceptual variant in geometric design, supporting the proposed validation-driven approach based on the analogy in entry mechanisms. It was used as a reference to validate the simulated two-lane roundabout model due to the similarities in vehicle approach and navigation. Entry mechanisms in roundabouts or turbo roundabout approaches include the following [12,13,27,29]: single-

lane entry conflicts with a single circulatory lane, as is typical in the approach to a single-lane roundabout and a turbo roundabout with one circulatory lane (e.g., S-W approach at the knee-turbo roundabout in Figure 5b); single-lane entry with two circulating lanes, where one entry lane conflicts with both circulating lanes (the driver enters the roundabout and selects the lane based on the desired exit) [12,14]; two-lane entry with a single circulatory lane is used in two-lane roundabouts or turbo roundabouts, where an inside circulatory lane is added at one approach (e.g., the E-S approach for the knee turbo roundabout in Figure 5b) or at approaches aligned in the same direction (e.g., basic or egg turbo roundabouts) [14,27]; two-lane entry with two circulatory lanes where drivers preselect the lane before entering and then maneuver towards the desired exit in a two-lane roundabout (e.g., Figure 5a) or turbo roundabouts (e.g., N-E and W-N approaches at knee-turbo roundabout in Figure 5b).

Operationally, turbo roundabouts' spiral geometry and lane dividers require drivers to choose the correct lane prior to entry to ensure proper exiting. At the two-lane exits, drivers in the inside lane turn to exit similarly to those in two-lane roundabouts. However, turbo roundabouts eliminate the need for inside-lane drivers to cross the outside lane by design, physically preventing this crossing and requiring drivers in the outside lane to exit directly [28,29]. However, the circular design of roundabouts and turbo roundabouts helps control vehicle speeds, enhancing safety and traffic flow during all movement stages [12,27]. Such design characteristics facilitate predictable traffic patterns and similar operational dynamics. In both the knee-turbo roundabout and the two-lane roundabout shown in Figure 5, drivers follow comparable entry rules, such as yielding to circulating traffic and selecting appropriate lanes based on their intended direction. This consistency enhanced the effectiveness of validating the simulated models, as vehicle behavior can be expected to align at both roundabouts due to their similar geometries and traffic operations.

In the selected approach for analysis (i.e., the W-N approach in Figure 5a,b), the left lane was conflicted by two circulating traffic flows, while the right lane intersected with only one flow. Consequently, drivers entering from the right lane used the outer circulating lane, while those entering from the left lane traveled in the inner circulating lane at both roundabouts. As a result, the right lane of the two-lane roundabout effectively functioned as a de facto right-turn lane, conflicting with one circulating lane. This setup enabled a comparative operational analysis between the two designs. Overall, this validation approach provided an additional method for assessing the accuracy of the intersection calibration.

The passage highlights opportunities for CAVs and V2V communication at roundabouts [1,13]. It notes that for a VHD waiting to enter, routing decisions of conflicting vehicles remain uncertain until the vehicle commits to entering, circulating, or exiting, which can lead to delays and reduced capacity. When both yielding and incoming vehicles are CAVs, V2V communication enables them to share routing information, potentially enhancing flow and efficiency, as a CAV approaching a roundabout can detect incoming vehicles through line-of-sight sensors or V2V communication. The entering CAV prioritizes the closest approaching vehicles, assesses for route conflicts, and can enter before the incoming vehicle signals its intention to circulate or exit [13,27]. If the first vehicle in the approaching stream is not a CAV or if route conflicts exist, the CAV's behavior is governed by gap acceptance criteria [12]. In this context, path guidance strategies, including advanced pavement markings, dynamic signage, lane delineation, and enhanced lighting, improve the safe navigation of CAVs on curved layouts by reducing conflicts and congestion [1,12].

2.2. Intersection Operation Analysis

Beginning with a baseline scenario featuring only VHDs, five traffic settings were simulated in Aimsun, using increments of 20% CAVs. The baseline traffic setting contained 100% VHDs and 0% CAVs, while the subsequent traffic settings included (1) 80% VHDs

and 20% CAVs, (2) 60% VHDs and 40% CAVs, (3) 40% VHDs and 60% CAVs, (4) 20% VHDs and 80% CAVs, and (5) 0% VHDs and 100% CAVs. The research began by defining micro-simulation models in Aimsun, focusing on the conceptualized intersection layouts and traffic settings. The calibration process concentrated on the signalized intersection and the roundabout models by leveraging, in this latter case, the analogy of yield negotiation at the entries of both roundabouts shown in Figure 5. Validation used the knee-turbo roundabout as a control scheme to assess the calibration accuracy. Due to the absence of observed data for vehicles with high automation levels, RCFs were developed for both the signalized intersection and the two-lane roundabout to serve as target data. The equations in Table 1 were used to create RCFs that reflect varying CAV-MERs at the intersection level [13].

Table 1. Equations for signalized intersections and roundabout capacity calculation.

Intersection Type	Capacity Formula	Parameters Description	
Signalized intersection	$C_{CAVs} = \frac{G \cdot N_l \cdot S_{fr,\ CAVs}}{c}$	C_{CAVs}: entry capacity (veh/h); G: the effective green time (s); N_l is the number of lanes in a lane group; $S_{fr,CAVs}$: the saturation flow rate (veh/h/ln); and c: the total cycle length (s).	(1)
	$S_{fr,CAVs} = S_b \cdot \prod_{i=1}^{n} f_i$	$S_{fr,CAVs}$: the saturation flow rate (veh/h/ln); S_b: the base saturation flow rate (veh/h/ln); f_i: the correction factors.	(2)
Roundabout	$C_{e,CAVs} = f_{(a)} \cdot a \cdot e^{-f_{(b)} \cdot b \cdot Q_c}$	$C_{e,CAVs}$: CAVs' capacity (pc/h); Q_c: circulating flow rate (pc/h); a: intercept parameter (equal to 1380 pc/h for the right entry lane; 1350 pc/h for the left entry lane); b: slope parameter (equal to 0.00102 and 0.00092 for the right and left entry lanes, respectively); and $f_{(a)}$ and $f_{(b)}$: correction factors for the parameters a and b, respectively [13].	(3)

Model parameters were iteratively refined based on the alignment of simulated outputs with the RCFs during the calibration process. The green time and the traffic light cycle length in Table 1 (see Equation (1)) were collected in the field at the signalized intersection, while the saturation flow rate was calculated according to [13]. The base value for the saturation flow was initially set at 1900 pc/h, but this was corrected by factors (f_i) that consider specific characteristics of the subject intersection, such as lane width, turning movements, heavy vehicles, and CAVs in traffic (see Equation (2) in Table 1).

As the CAV-MERs changed, the base saturation flow rate for through movements also varied, while the saturation flow rate for left turns was adjusted with an additional correction factor based on the CAV-MERs. Modifications in CAV capacity for right turns were consistent with [13]. The surfaces in Figure 6 illustrate the RCFs with varying CAV-MERs at the roundabout and the signalized intersection. Specifically, Figure 6a displays the RCF of the left entry lane (LEL) at the roundabout, while Figure 6b shows the RCF of the right entry lane (REL) at the roundabout. Meanwhile, Figure 6c shows the RCF of the exclusive left-turn lane (L) at the signalized intersection as the green time increased, while Figure 6d shows the RCF of the shared right-turn and through lane (R&T) at the signalized intersection as the green time increased, highlighting how effective green time varied in response to different CAV-MERs while keeping the total cycle length constant.

2.3. Modeling Intersection Case Studies in AIMSUN to Evaluate the Validation-Driven Approach

Aimsun micro-simulator (Version 20) was used to assess the impact of different intersection layouts on the operational effectiveness of CAVs mixed with VHDs [17]. Given that lane divisors (e.g., curbs or road markings) are used to separate each lane at the knee-turbo

roundabout, the functionality with curbs was simulated to ensure entry lane preselection and prevent lane changes. Micro-simulation models were defined based on the geometrical features of the conceptualized intersections, simulating traffic data and settings using origin–destination (O−D) matrices.

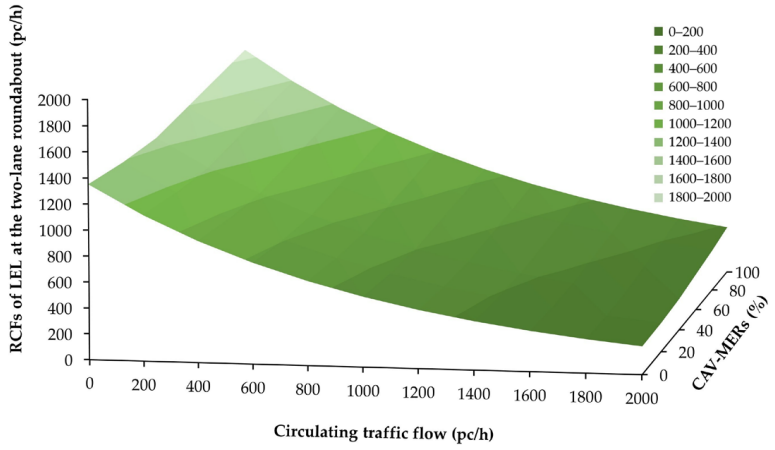

(**a**)

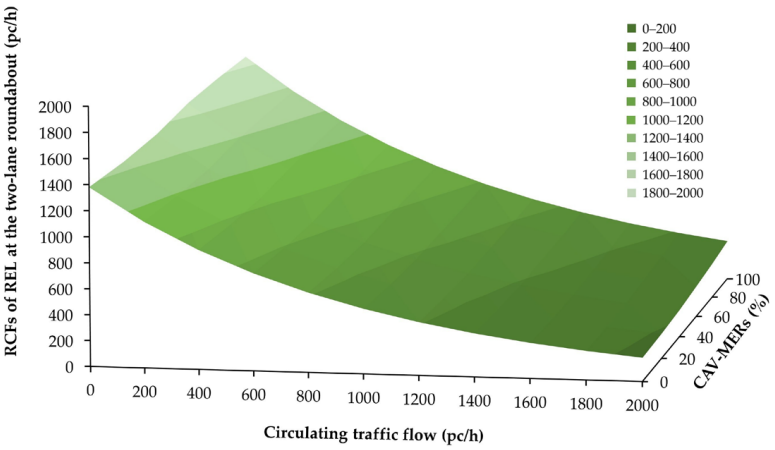

(**b**)

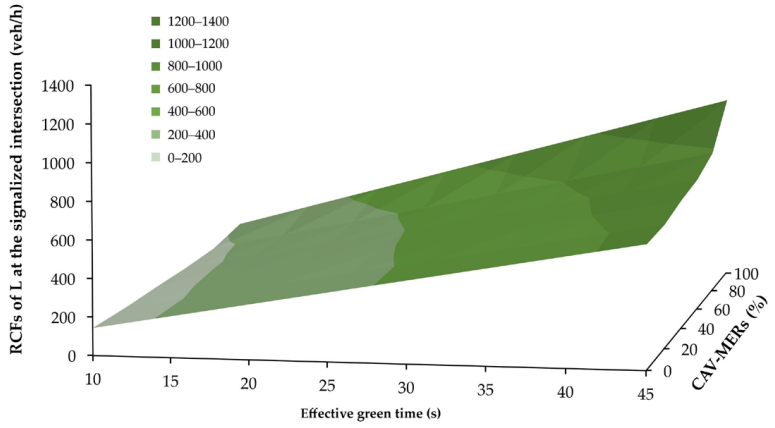

(**c**)

Figure 6. *Cont.*

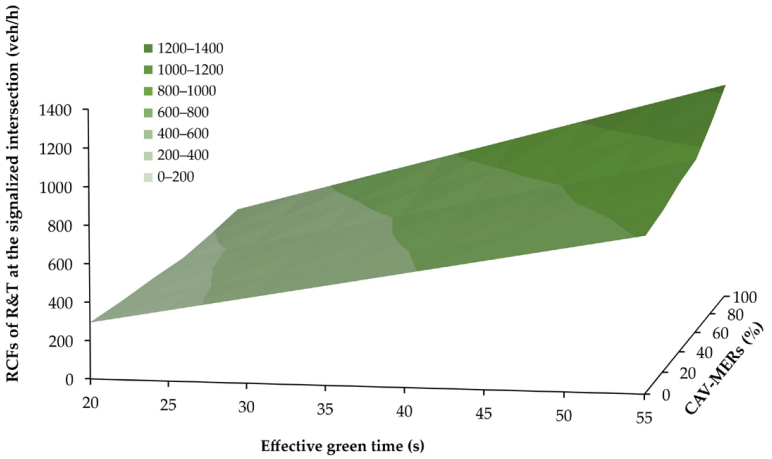

(**d**)

Figure 6. RCFs with varying CAV-MERs for (**a**) the reference left entry lane (LEL) capacity at the two-lane roundabout; (**b**) the reference right entry lane (REL) capacity at the two-lane roundabout; (**c**) the reference exclusive left-turn lane (L) group capacity at the signalized intersection as the green time increased; and (**d**) the reference shared right-turn and through lane (R&T) group capacity at the signalized intersection as the green time increased. Note: the acronyms are provided in the legend.

Based on the mentioned traffic settings, the total traffic matrix was divided into two distinct matrices: one matrix represented a specific percentage (x) of CAVs, while the other matrix contained the remaining percentage (1 − x) of VHDs. For every intersection, an appropriate type of traffic control was systematically assigned: give-way signals were allocated to each entry lane at roundabouts, while a time control plan was developed at the signalized intersection based on comprehensive field observations and data analysis. Detectors were installed on specific road sections to continuously monitor changes in entry capacity. Ten one-hour simulation trials with only VHDs were executed to assess Aimsun's accuracy in replicating the observed traffic flows.

The simulation results emphasized the need to calibrate the model parameters, revealing a percentage difference of approximately 12% between the simulated and field data. Assuming high communication reliability, V2V communication for CAVs was enabled through the CACC module, allowing for information exchange to minimize the distance to the vehicle ahead and improve overall traffic efficiency and safety [17,30]. The Gipps' car-following model analyzed vehicle behavior by measuring the spacing and timing between cars [31]. In turn, the lane-changing model assessed the available gaps for safe lane changes, while gap-acceptance models evaluated driver decision-making at intersections based on kinematic parameters, determining the feasibility of maneuvers in varying traffic conditions.

Before booting the calibration process, a sensitivity analysis was conducted to evaluate how changes in model parameters for each intersection affected the simulation results. Regardless of the intersection model considered, the sensitivity analysis primarily involved global parameters affecting all vehicles in the network and specific vehicle class parameters targeting distinct road user categories. Figure 7 summarizes the sensitivity analysis results for the case study, illustrating the variation of entering traffic within the range of the most sensitive parameter values.

The most sensitive parameters were then calibrated by iteratively adjusting their values to closely align the simulated capacity data with the RCFs, ensuring a more accurate representation of traffic behavior in the model. Notably, among the global modeling parameters, the reaction time of moving vehicles was identified as the most sensitive across all defined models.

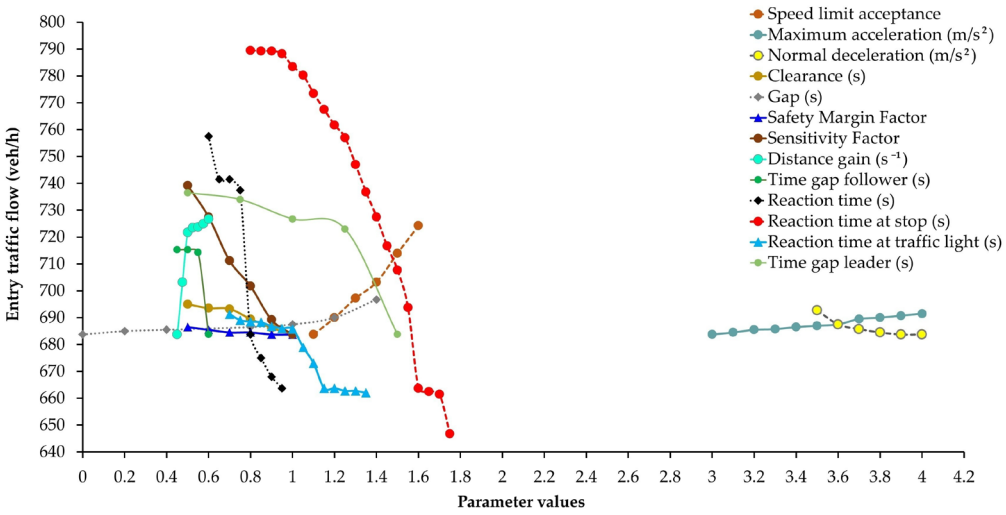

Figure 7. The graphic development of the sensitivity analysis of the model parameters.

This sensitivity also applied to reaction times at stops and traffic lights, impacting vehicles in stationary conditions significantly. The reaction time, measured in seconds, is a parameter in car-following models that reflects the time taken by a vehicle to respond to speed variations of the vehicle ahead [17]. If fixed, this parameter aligns with the simulation step for all users' classes; however, it can also be defined as a variable based on a probability function tailored to the specific characteristics of each user class, enhancing model accuracy.

The reaction time at a stop refers to the duration a queuing vehicle takes to initiate movement once the preceding vehicle restarts. Similarly, the reaction time at traffic lights occurs at signalized intersections and represents the duration taken by the first vehicle at the stop line to accelerate in response to the green signal.

Table 2 shows the calibrated values of the model parameters for the signalized intersection and the two-lane roundabout.

Table 2. Calibrated values of the model parameters for the signalized intersection and the two-lane roundabout.

Model Parameters	Default Values	Tuned-up Model Parameter Values							
		Signalized Intersection				Two-Lane Roundabout			
		L		R&T		LEL		REL	
		VHDs	CAVs	VHDs	CAVs	VHDs	CAVs	VHDs	CAVs
Speed limit acceptance	1.10	1.30	1.60	1.30	1.60	0.97	1.10	1.00	1.10
Maximum acceleration (m/s^2)	3.00	3.20	3.40	3.20	3.40	3.00	4.00	3.00	4.00
Normal deceleration (m/s^2)	4.00	4.00	3.50	4.00	3.50	4.00	4.00	4.00	4.00
Clearance (s)	1.00	1.00	0.50	1.00	0.50	1.00	1.00	1.00	1.00
Gap (s)	0.00	0.00	0.00	0.00	0.00	1.33	0.00	1.58	0.00
Safety Margin Factor	1.00	1.00	1.00	1.00	1.00	1.00	0.50	1.00	0.50
Sensitivity Factor	1.00	1.00	1.00	1.00	1.00	1.00	0.50	1.00	1.00
Distance gain (s^{-1})	0.45	0.45	0.60	0.45	0.60	0.45	0.45	0.45	0.45
Time gap leader (s)	1.50	1.50	0.50	1.50	0.50	1.50	1.50	1.50	1.50
Time gap follower (s)	0.60	0.60	0.50	0.60	0.50	0.60	0.60	0.60	0.60
Reaction time (s)	0.80	0.85 [1]	0.62 [2]	0.80 [1]	0.60 [2]	0.95 [1]	0.67 [2]	0.86 [1]	0.63 [2]
Reaction time at stop (s)	1.20	1.75 [1]	1.06 [2]	1.60 [1]	0.82 [2]	1.20	1.20	1.20	1.20
Reaction time at traffic light (s)	1.60	1.36 [1]	1.02 [2]	1.20 [1]	0.73 [2]	1.60	1.60	1.60	1.60

Note: The reaction time is the weighted mean of the corresponding values based on CAV-MER, with each MER used as a weight: [(1)] 0% of CAVs, [(2)] 100% of CAVs. Based on my own research using the default data presented in [17].

The parameters for calibrating both VHDs and CAVs included speed limit acceptance, which refers to the driver's compliance with speed limits, and maximum acceleration (m/s^2), representing the highest acceleration that a vehicle can achieve within each network model, consistent with the geometry or traffic control mode of the intersection type. The speed acceptance values greater than one mean that vehicles can assume maximum speeds exceeding the speed limit, otherwise below the speed limit, thus denoting a more cautious driving behavior. Consistent with the traffic control mode, VHDs and CAVs at signalized intersection assumed a decisive driving behavior, since both the speed limit acceptance and maximum acceleration parameters resulted in higher values than the default values of 1.10 and 3.00 m/s^2, respectively (see Table 2). On the contrary, the speed limit acceptance was set below the default threshold for the VHDs at the two-lane roundabout, while the maximum acceleration was maintained as the default value. Differently from [11], although the curved geometry forced CAVs to adhere to the speed limit at the examined two-lane roundabout, they adopted an assertive driving behavior, assuming maximum acceleration values higher than the default one, thanks to the V2V communication. Further parameters that were highly sensitive in the context of CAVs operating at the signalized intersection included normal deceleration (m/s^2) and clearance (s). The former denotes the maximum deceleration employed by any vehicle in typical driving situations, while the latter indicates the distance between two stationary vehicles. These two parameters were found to have less effect on the calibration of both vehicle classes in roundabouts, where the dominant factor influencing driving behavior is the effect induced by the curvilinear geometry of the layout [11]. A parameter typically tuned for CAVs operating at roundabouts is the safety margin factor, which determines vehicle priorities at intersections [11,17]. It was set to 0.50 for both roundabout entry lanes, replacing the default value of 1.00, while the default value remains in effect for the cautious driving behavior of VHDs at roundabout entry lanes [11]. The adjusted value of the safety margin employed here is consistent with the recommendations by Aimsun [17], where this parameter can be adjusted for a specific maneuver to reflect the road geometry under examination. The set of modeling parameters for the traffic roundabout scenarios with CAVs included the sensitivity factor, which relates to the distance between vehicles based on the deceleration assessments of the following vehicle to estimate the leader's deceleration, collectively modeling CAVs' driving behavior at the roundabout. Aimsun [17] allows you to adjust the vehicle headway distribution to indicate cautious driving or assertive driving. Therefore, a sensitivity factor greater than 1.00 indicates cautious driving, while a value below 1.00 reflects assertive driving (see Table 2). The value tuned for CAVs was a compromise to simulate changes in driving behavior or interactions among different vehicles on curved paths to evaluate CAV driving skills in mixed traffic conditions [17]. This parameter was set to 0.50 for the LEL, replacing the default value of 1.00, while the default value remains in effect for the cautious driving behavior of VHDs at roundabout entry lanes. In turn, the gap parameter, which measures the distance in seconds between the front bumpers of consecutive vehicles, was calibrated for VHDs as representative of their behavior at roundabouts, while the default value remains in effect for CAVs.

In CAV modeling, distance gain (s^{-1}), time gap leader (s), and time gap follower (s) were used to represent the spatial and temporal distances between vehicles equipped with the CACC module while queuing. Similar considerations were found in [2,32] to approximate the driving behavior of CACC-CAVs during cruising. Aimsun allows the analyst to set the distribution of VHDs and the percentage of CACC-CAVs in the respective tabs [17]. Consequently, the aforementioned parameters—characteristic of the CAV guide—have been kept at their default values for VHDs. Additionally, these parameters were found to have a greater influence on signalized intersections than on roundabouts, where

the dominant factor affecting driving behavior is primarily governed by the curvilinear geometry of the layout and its smoothing effect.

Finally, the calibrated reaction times are shown in Table 2. In CAV modeling, the reaction time is set to 0.62 s for the L group and 0.60 s for the R&T group, while it is set to 0.67 s for the LEL and 0.63 s for the REL, replacing the default value of 0.80 s across all lanes. Additionally, the reaction times at stop and traffic lights commonly tuned for signalized intersections, were maintained at their respective default values for both CAVs and VHDs in both entry lanes at roundabouts [17].

The calibration results in Table 2 highlight the assertiveness of CAVs and VHDs at the signalized intersection, where speed acceptance and maximum acceleration values exceeded their respective default thresholds [16]. Conversely, for VHDs at the roundabout, the speed acceptance value fell below the default value, while the reaction time surpassed the predefined threshold, indicating slightly risk-averse behavior. CAVs demonstrated a more decisive driving attitude at the examined roundabout, reacting more readily to the leader's actions with higher acceleration than default values and slower reaction times and safety margins below the thresholds. The tuned CACC-CAV parameters enabled these vehicles to use intra-vehicle communication more effectively, allowing them to drive decisively at the signalized intersection compared to the roundabout, which typically accommodates smoother traffic flow.

The Geoffrey index (GEH) measured the deviation between simulated data and RCFs, aiming for discrepancies of less than 5 in at least 85% of cases [16]. The percentage difference between the two datasets indicated calibration success and confirmed the validity of the calibration process. The GEH index was used in the calibration of the two-lane roundabout by comparing simulated data with the RCFs as CAV-MERs increased, achieving over 90% accuracy for the LEL and REL. Additionally, the accuracy of the signalized intersection calibration was determined by a 5% percentage difference between simulated capacity and RCFs.

Table 3 presents statistics for the lanes' groups (i.e., L and R&T) at the signalized intersection. The t-statistic indicated no significant difference between the means of simulated data and RCFs, while the F-statistic confirmed equal sample variances. The root mean squared normalized error (RMSNE) demonstrated close alignment between simulated data and capacity values, corroborating the calibration process and the models' effectiveness in replicating the examined phenomenon. Similar promising results were observed for both lanes (i.e., LEL and REL) of the roundabout, as shown in Table 4.

Table 3. Summary statistics comparing the simulated capacity values and RCFs for different CAV-MERs at the signalized intersection.

Statistics	**CAV-MERs by Lane Group (%)**											
	0		**20**		**40**		**60**		**80**		**100**	
	L	**R&T**	**L**	**R&T**	**L**	**R&T**	**L**	**R&T**	**L**	**R&T**	**L**	**R&T**
Mean $_1$	362.22	566.67	371.00	594.22	395.33	648.22	417.44	690.22	449.33	760.11	551.78	858.33
s.e. $_1$	62.04	61.86	62.78	64.70	64.66	69.84	70.77	72.19	74.85	79.13	91.94	89.39
Mean $_2$	367.54	574.80	371.21	605.05	393.27	650.43	407.97	680.68	444.72	771.44	573.36	877.32
s.e. $_2$	60.66	60.91	61.27	64.12	64.91	68.93	67.33	72.13	73.40	81.75	94.63	92.97
95% c.i. *	(−189.3, 178.6)	(−192.2, 175.9)	(−186.2, 185.7)	(−203.9, 182.4)	(192.2, 196.3)	(−210.4, 205.7)	(−197.6, 216.6)	(−206.7, 226.0)	(−217.6, 226.9)	(−252.6, 229.9)	(−301.3, 258.1)	(−292.4, 254.4)
t-value	−0.06	−0.09	−0.002	−0.12	0.02	−0.02	0.10	0.09	0.04	−0.10	−0.16	−0.15
t-critical	2.12	2.12	2.12	2.12	2.12	2.12	2.12	2.12	2.12	2.12	2.12	2.12

Table 3. *Cont.*

Statistics	CAV-MERs by Lane Group (%)											
	0		20		40		60		80		100	
	L	R&T	L	R&T	L	R&T	L	R&T	L	R&T	L	R&T
$p(\alpha)$value	0.95	0.93	0.98	0.91	0.98	0.98	0.92	0.93	0.96	0.93	0.87	0.88
F-statistic	1.05	1.03	1.05	1.02	1.01	1.03	1.10	1.01	1.04	1.07	1.06	1.08
F-critical	3.44	3.44	3.44	3.44	3.44	3.44	3.44	3.44	3.44	3.44	3.44	3.44
F-prob	0.95	0.97	0.95	0.98	0.99	0.97	0.89	0.98	0.96	0.93	0.94	0.91
RMSNE	0.04	0.02	0.02	0.03	0.02	0.01	0.03	0.02	0.02	0.02	0.04	0.02

* c.i. stands for confidence interval. Note: Mean $_{1,2}$ (s.e. $_{1,2}$) are referred to each mean value and standard error of the two groups of data (namely the simulated data and RCFs).

Table 4. Summary statistics comparing the simulated capacity values and RCFs for different CAV-MERs at the two-lane roundabout.

Statistics	CAV-MERs by Entry Lane (%)											
	0		20		40		60		80		100	
	LEL	REL	LEL	REL	LEL	REL	LEL	REL	LEL	REL	LEL	REL
Mean $_1$	774.50	821.69	745.93	876.45	786.75	943.93	881.15	1046.77	980.67	1128.53	1067.83	1211.58
s.e. $_1$	57.99	61.22	56.60	63.20	58.35	65.86	62.70	71.86	67.64	72.67	71.40	72.09
Mean $_2$	731.11	810.41	738.00	883.28	799.77	954.29	887.45	1019.71	1001.66	1060.85	1107.11	1115.14
s.e. $_2$	67.97	72.37	66.28	75.90	68.27	77.33	72.47	79.67	78.52	79.79	85.92	77.71
95% c.i. *	(−135.3; 222.0)	(−178.8; 201.4)	(−165.9; 181.8)	(−204.8; 191.2)	(−192.2; 166.1)	(−214.0; 193.3)	(−197.4; 184.8)	(−188.1; 242.2)	(−227.7; 185.7)	(−148.7; 284.1	(−262.1; 183.5)	(−116.1; 309.0)
t-value	0.51	0.12	0.13	0.07	0.15	0.10	0.11	0.25	0.20	0.63	0.35	0.91
t-critical	2.000	2.006	1.995	2.007	1.995	2.006	1.995	2.006	1.995	2.005	1.995	2.005
$p(\alpha)$value	0.63	0.91	0.93	0.95	0.88	0.92	0.95	0.80	0.84	0.53	0.73	0.37
F-statistic	1.37	1.40	1.37	1.44	1.37	1.38	1.34	1.23	1.35	1.21	1.45	1.16
F-critical	1.76	1.91	1.76	1.91	1.76	1.91	1.76	1.91	1.76	1.91	1.76	1.91
F-prob	0.38	0.40	0.35	0.35	0.36	0.41	0.40	0.60	0.38	0.63	0.28	0.70
RMSNE	0.13	0.16	0.09	0.14	0.07	0.10	0.07	0.08	0.06	0.11	0.07	0.13

* c.i. stands for confidence interval. Note: Mean $_{1,2}$ (s.e. $_{1,2}$) are referred to each mean value and standard error of the two groups of data (namely the simulated data and RCFs).

The scatter plots in Figure 8 drive the validation of the analogy in entry mechanisms for the roundabout and knee-turbo roundabout (W-N approach). By way of example, Figure 8a displays capacity data for the LEL, and Figure 8b shows the REL with 40% CAVs and 60% VHDs. The narrow prediction intervals and high R^2 values observed across the different cases indicated a strong positive correlation between the datasets for both roundabout types, thereby supporting the extension of the two-lane roundabout calibration to the knee-turbo roundabout model.

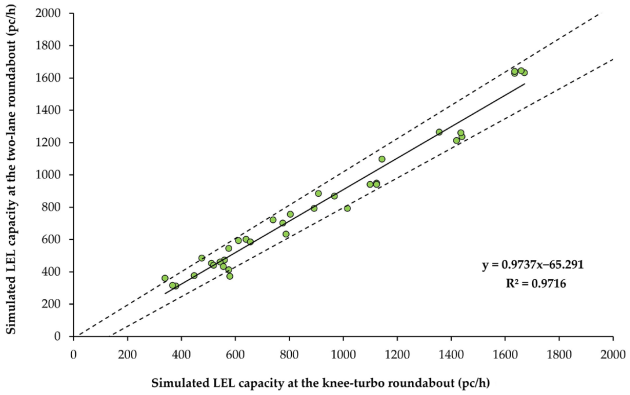

(**a**)

Figure 8. *Cont.*

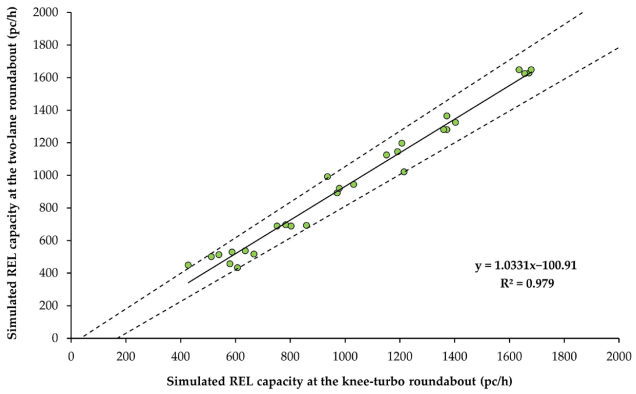

(**b**)

Figure 8. Scatter plots at 40% CAVs and 60% VHDs comparing the capacities of the simulated two-lane and the knee-turbo roundabouts for (**a**) the left entry lane (LEL); (**b**) the right entry lane (REL). Note: the acronyms are provided in the legend.

3. Results of the Simulation Experiments

A microsimulation approach was deemed to assay the efficiency of CAVs and VHDs across different intersection layouts and traffic scenarios as part of the move towards automated smart mobility. CAVs were assumed to operate in either realistic traffic scenarios with perfect communication conditions [30]. Entry capacity (pc/h), delay (s), and travel time (s) were selected as the operational performance metrics for simulation trials across six traffic scenarios with varying CAV-MERs. Capacity represents the maximum number of vehicles entering a road section, while delay indicates the difference between the expected travel time through the intersection and the actual time experienced by users without the intersection, averaged across all vehicles. Additionally, travel time reflects the average duration spent by all vehicles moving through the network [13,17].

Focusing on the W-N approach in Figures 2 and 5, Figure 9 compares the knee-turbo roundabout, two-lane roundabout, and signalized intersection regarding the percentage differences in entry capacity by entry lane or lane group (i.e., LEL and L capacities in Figure 9a and REL and R&T capacities in Figure 9b) between the baseline setting with 0% CAVs and traffic settings with progressively increasing CAV-MERs.

Overall, the simulation results showed that operational conditions, from low to high conflicting flows approaching entry capacity, improved with increasing CAV-MERs across all examined intersections. The bar graph in Figure 9a concerning LEL and L capacities illustrates higher percentage increases in the LEL capacity at roundabouts for CAV-MERs ranging from 20% to 60%, compared to traffic settings with CAV-MERs of 80% and above. In turn, with CAV-MERs of 80% the signalized intersection exhibited a rapid increase in percentage capacity of approximately 34% for the considered lane group, followed by the corresponding entry lanes of the knee-turbo and two-lane roundabouts, with capacity growths of 27% and 26%, respectively. When only CAVs travelled on the network (see Figure 9a), the considered lane group at the signalized intersection showed a percentage capacity growth of 58% compared to the baseline scenario with only VHDs, followed by the knee-turbo roundabout with an entry lane capacity growth of 41%. Meanwhile, the LEL capacity at the two-lane roundabout maintained a similar growth trend as observed in the previous cases.

In turn, Figure 9b concerning REL and R&T capacities displays the percentage increase compared to the baseline scenario at the three examined intersections. The bar graph in Figure 9b indicates that the two-lane roundabout experienced a higher percentage REL capacity growth compared to the R&T capacity at the signalized intersection for CAV-MERs

ranging from 20% to 40%. Conversely, for CAV-MERs of 60% to 100%, the signalized intersection exhibited a more pronounced increase in capacity compared to the roundabouts, where operational performance generally depends on traffic flow matrices [12,33]. Moreover, the L group at the signalized intersection, designed for a specific traffic movement, generated higher capacity increments compared to the R&T, particularly at elevated CAV-MERs (Figure 9a,b). The presence of curbs in the knee-turbo roundabout may enhance LEL capacity, particularly at high CAV-MER values, facilitating improved traffic flow and movement efficiency; however, these curbs can also hinder the capacity increase for the REL case as CAV-MERs rise by preventing traffic from spreading across two lanes of the circulatory roadway. However, the presence of traffic lights, which eliminate the yielding negotiation process, allows for higher capacity compared to the baseline scenario, particularly when CAV-MERs reach 100%.

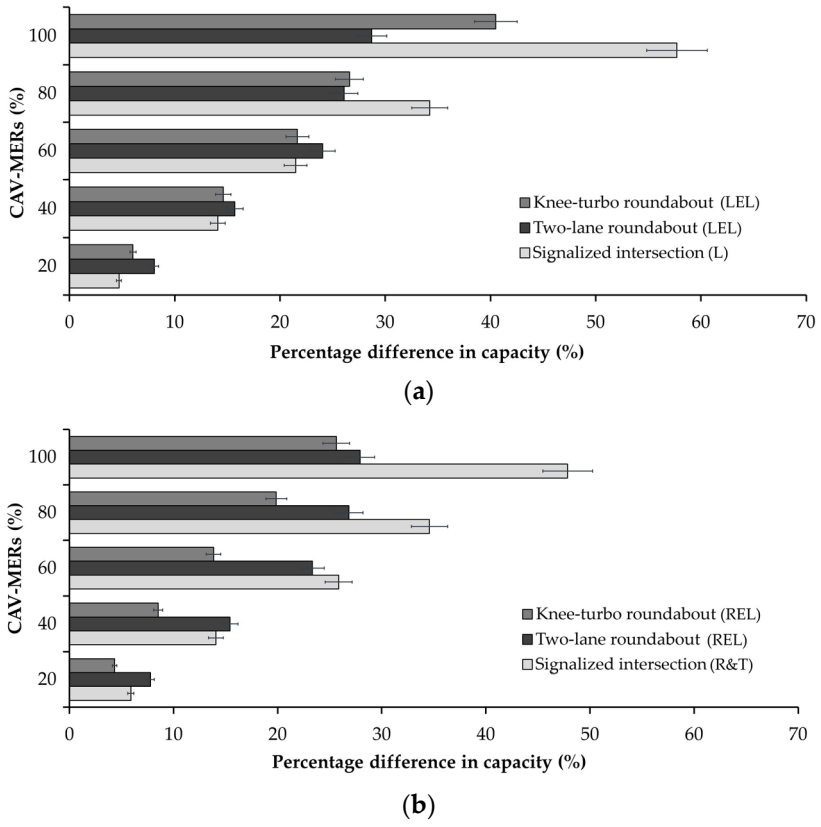

Figure 9. Comparison among the knee-turbo roundabout, two-lane roundabout, and signalized intersection in terms of percentage differences in capacity (pc/h) across various CAV-MERs for (**a**) the left-entry lanes (LELs) of two-lane and knee-turbo roundabouts and exclusive left-turn lane (L) of the signalized intersection; (**b**) the right-entry lanes (RELs) of two-lane and knee-turbo roundabouts and the shared right-turn and through lane (R&T) of the signalized intersection. Note: the acronyms are provided in the legend.

Based on traffic data collected in the field for the signalized intersection, an unbalanced traffic matrix was also used to simulate undersaturated conditions at the conceptualized intersections. Figure 10 displays a comparison among the three intersections (i.e., LEL and L delays in Figure 10a and REL and R&T delays in Figure 10b), highlighting the percentage differences in delay (s) for the CAV-MERs. The figure illustrates a larger percentage reduction in delay for both entry lanes at the knee-turbo roundabout compared to other intersections. The LEL delay at the knee-turbo roundabout in Figure 10a decreases by 40% to 65%, with CAV-MERs ranging from 40% to 100%. Similarly, the REL delay in Figure 10b decreases by 9% to 46%, with CAV-MERs ranging from 20% to 100%.

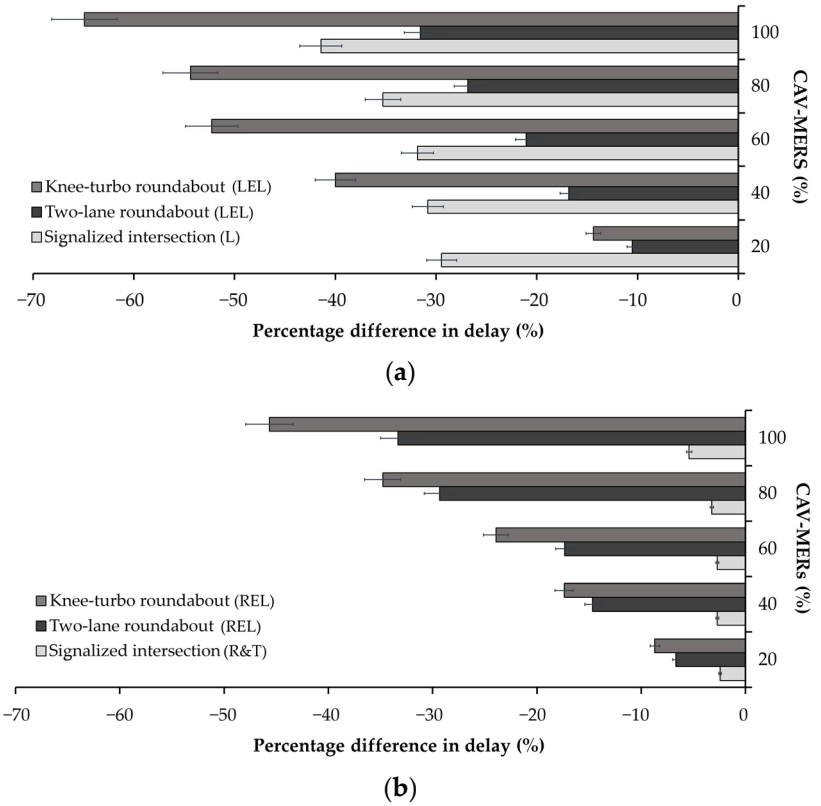

Figure 10. Comparison among the knee-turbo roundabout, two-lane roundabout, and signalized intersection in terms of percentage differences in delay (s) across various CAV-MERs for (**a**) the left-entry lanes (LELs) of the two-lane and knee-turbo roundabouts and the exclusive left-turn lane (L) of the signalized intersection; (**b**) the right-entry lanes (RELs) of the two-lane and knee-turbo roundabouts and the shared right-turn and through lane (R&T) of the signalized intersection.

The travel time trends for the entry lanes are illustrated in Figure 11 (i.e., LEL and L travel times in Figure 11a and REL and R&T travel times in Figure 11b). Overall, as CAV-MERs increase, the knee-turbo roundabout demonstrated a significant percentage reduction in travel time for both entry lanes compared to the other intersections across nearly all traffic settings. Figure 11a indicates that, for a CAV-MER of 20%, the signalized intersection experienced a percentage decrease in L travel time of 22%, compared to 10% for the corresponding entry lane in the knee-turbo roundabout. Percentage decreases in travel time of approximately 23% were observed for the considered lane (LEL) at the knee-turbo roundabout and lane group (L) at the signalized intersection for a CAV-MER of 40% (see Figure 11a). Additionally, the percentage reduction in travel time compared to the baseline scenario of VHDs is more pronounced for the REL at the knee-turbo roundabout, fluctuating from 7% to 31% for CAV-MERs starting from 20% onwards, followed by the REL at the two-lane roundabout and the R&T signalized intersection (Figure 11b).

Despite the similar decreases in delay and travel times across the three intersections, the knee-turbo roundabout geometry had a greater impact on the LEL performance than on the REL one; similarly, at the signalized intersection, the same effect was observed but differed by entry lane or lane group (i.e., L compared to R&T) due to lane group planning and the traffic control mode. In contrast, lane-changing behavior balanced the decrease in delay for both lanes of the two-lane roundabout.

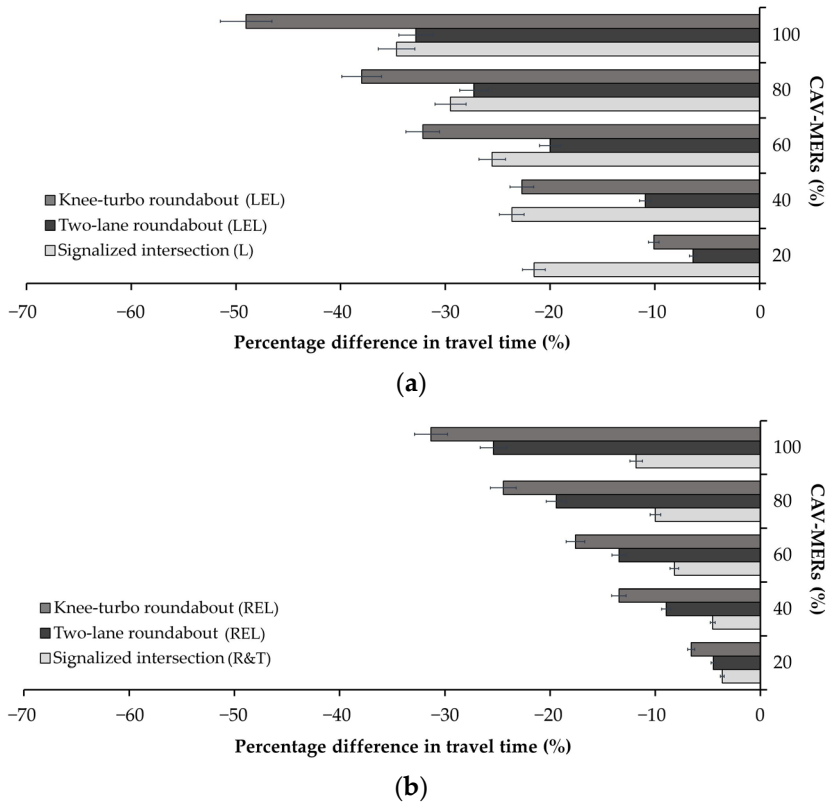

Figure 11. Comparison among the knee-turbo roundabout, two-lane roundabout, and signalized intersection in terms of percentage differences in travel times (s) across various CAV-MERs for (**a**) the left-entry lanes (LELs) of the two-lane and knee-turbo roundabouts and the exclusive left-turn lane (L) of the signalized intersection; (**b**) the right-entry lanes (RELs) of the two-lane and knee-turbo roundabouts and the shared right-turn and through lane (R&T) of the signalized intersection. Note: the acronyms are provided in the legend.

4. Discussion

Despite extensive discussions on CAV–infrastructure interaction, it is not always possible to directly transfer results obtained from other road infrastructures, such as road segments, to intersections [1,2,6,34]. A similar issue may arise concerning the specific objectives or methods proposed in the research—particularly related to the nodes of the road network—which can often hinder immediate comparisons, especially within the framework of smart cities [5,25,26]. Although the literature provides valuable insights, this is often because the design characteristics and vehicle dynamics of intersections and roundabouts are more complex, differing significantly from linear road sections due to conflict points or being influenced by the installation context. These aspects necessitate tailored approaches to design, management, and optimization [13]. Consequently, there is a proliferation of different case studies (e.g., [11,19,20,24,25]) which, while not always producing generalizable results, provide methodological pathways that can serve as valuable references for future research.

In this context, the study aimed to investigate how traffic scenarios involving connected and automated mobility can be channeled into the design of road intersections, thereby supporting the sustainable integration of smart vehicles into current and future road infrastructure.

Given that the current rate of replacing older vehicles with newer ones has not yet kept pace with advancements in the automotive industry, this study aims to support the real-world deployment of CAV technologies by emphasizing the importance of pilot studies to tackle practical and technical challenges. This approach aligns with the evolv-

ing needs of road engineering and underscores the critical role of ITS in facilitating this transition [1,2,34].

The results indicated significant traffic improvements with CAVs at the examined intersections (see Figures 9–11). As the transition to fully automated smart mobility advances, various traffic scenarios with increasing CAV-MERs were modeled in a microsimulation environment [17]. According to [13], due to the limited availability of smart vehicles for empirical analysis, RCFs for increasing CAV-MERs were developed to meet calibration requirements. To achieve optimal alignment between the simulated capacity outputs and RCFs, more sensitive driving behavior parameters were fine-tuned based on the sensitivity analysis for the signalized intersection and the two-lane roundabout, as illustrated in Figure 7. The calibration results in Table 2 indicated that CAVs and VHDs at the signalized intersection exhibited assertive behaviors, with speed acceptance and maximum acceleration exceeding thresholds. At the roundabout, VHDs demonstrated cautious behavior, with lower speed acceptance and reaction times above the thresholds. Conversely, CAVs at the roundabout displayed more decisive driving, reacting quickly with higher acceleration and lower reaction times and safety margins, facilitated by effective intra-vehicle communication through calibrated CACC-CAV parameters. Although the roundabout generally facilitated smoother traffic flow, V2V-enabled CAVs navigated the signalized intersection assertively. Statistics subsequently confirmed the accuracy of the calibration process (see Tables 3 and 4). The results were promising in matching the two datasets for each entry lane or lane group at the signalized intersection and two-lane roundabout, thereby addressing key question 1 in Section 1. As a result, the Aimsun models were considered carefully calibrated for replicating the studied phenomenon. A validation-driven approach was then proposed to assess the potential applicability of the two-lane roundabout calibration to the proposed knee-turbo counterpart, as both roundabouts featured similar entry mechanisms by approach. The proposed methodology ensured the reliability of the calibration results across two different roundabout configurations, as demonstrated by the scattergram analysis of the simulated capacity data for the calibrated roundabout models in Figure 8. This highlights the potential to extend the calibration of the two-lane roundabout to other intersection designs with similar entry mechanisms.

Three performance metrics were chosen to evaluate how intersection patterns affect the operational efficiency of CAVs across different traffic settings. Cross-referencing the conceptualized intersection solutions, the results underscored that CAV operation depends on both the intersection layout and the CAV-MERs, thereby enabling us to address key question 2 in Section 1. CAVs are more likely to accept smaller traffic gaps than VHDs, leading to increased entry capacity and improved delays and travel times as CAV-MERs rise.

Specifically, simulation results demonstrated greater percentage increases in capacity for the signalized intersection compared to roundabouts at high CAV-MERs, across both entry lanes and lane groups. This suggests that at CAV-MER levels of 60% or higher, signalized intersections can accommodate more vehicles more effectively than roundabouts, whose operational performance typically depends on traffic matrices [12,13,33] (see Figure 9). The results in Figure 9 align with those of [20], where a signalized intersection was simulated in Vissim [35] as a testbed, using traffic scenarios based on varying market penetration rates of smart vehicles mixed with VHDs. Specifically, increasing the proportion of CAVs—expected to receive information about upcoming traffic light states to adjust their speeds accordingly—was shown to enhance intersection capacity. Additionally, the study revealed that the greatest increase in lane group capacity occurred in a traffic stream composed entirely of CAVs [20]. However, potential lane changes at the two-lane roundabout—where vehicles can switch lanes based on available gaps—facilitated increased REL capacity compared to the knee-turbo scheme (see Figure 9b).

Conversely, analyzing the simulation outcomes of the intersections operating in undersaturated traffic conditions, the signalized intersection experienced a smaller reduction in delay and travel times than roundabouts as the number of CAVs in traffic increased [7,12] (see Figures 10b and 11b). This was more evident for the R&T than for the other lane group at the signalized intersection, due to the traffic setup in lane groups and the control mode. The results on percentage differences in travel time across various CAV-MERs are consistent with the findings of Mohebifard and Hajbabaie [24] at a single-lane roundabout in the United States. Although their study focused on trajectory control of CAVs, the authors [24] found that increasing the CAV-MERs from 20% to 100% reduced the travel times by 2.8% to 35.8%. Similar trends in vehicle delay times, compared to the case with 0% CAVs, were reported by [11,24] at single-lane and two-lane roundabouts, which were used as case studies to illustrate the methodologies proposed in each of these studies.

In this context, the research showed that CAV operations are affected by both the intersection layout and CAV-MERs. The signalized intersection outperformed roundabouts in capacity at high CAV penetration levels, while roundabouts offered better reductions in delay and travel times under undersaturated conditions (Figures 9–11). Although the journey time savings and delay time improvements observed in the simulation trials of the roundabout models are promising, they should be interpreted in the context of the traffic arrival distribution and the underlying hypotheses of the study. The simulation results also demonstrated that the intersection scheme affects connected and automated driving performance, with certain layouts showing a tendency to enhance the operational efficiency of smart mobility during the transition to full CAV adoption. However, due to the current absence of high-automation-level CAVs in traffic—limiting the availability of empirical data—the findings are inevitably influenced by the assumptions underlying the study. This is also consistent with the simulation results reported by [19], which indicated that, among intelligent vehicles, CACC-CAVs can outperform other intelligent vehicle systems in mixed traffic flows with VHDs at fixed and actuated signalized intersections. Additionally, simulations demonstrated reductions in average delay from 20% MPR, with performance improvements measured at actuated signal-controlled intersections under high traffic demand [19].

Although the impact of CAVs on traffic safety and efficiency in scenarios involving imperfect communication warrants further investigation [30], improvements in throughput and delays were documented by [25] in a single-lane roundabout case study used to demonstrate the capabilities of an expert system for managing conflicting vehicles. Fully CAV traffic increased the roundabout's capacity by 58–73%, and an optimized coordination strategy significantly reduced delays compared to VHDs. However, the authors emphasized the necessity of accounting for greater variability in CAV behaviors across different road scenarios to ensure that the results are broadly applicable.

Therefore, in response to the third question in Section 1, the authors emphasize that while the proposed validation-driven approach aided the comparison of different intersection design solutions based on the analogy of entry mechanisms by approach, a broader array of case studies should be further investigated to establish a comprehensive general performance criterion for effective comparison. Additionally, analyzing a larger series of intersection schemes and control modes would enhance the identification of context-specific factors, which could be incorporated into a robust performance criterion based on similar entry mechanisms. This also emphasizes the importance of developing novel assessment approaches for integration into practical roadway design workflows.

Based on the above, this research enhances understanding of how connected and automated mobility interacts with different intersection designs, emphasizing the importance of layout, operational parameters, and accurate behavioral modeling in traffic system analysis.

These findings help establish a theoretical framework linking CAV-MERs, intersection design features, and operational efficiency, offering a reference for future studies in ITS and mobility modeling under evolving traffic conditions.

Practically, the study offers valuable insights for transportation planners and road engineers, illustrating how various intersection configurations respond to increasing CAV market shares. The results suggest that signalized intersections may be better suited to accommodate higher levels of CAV penetration—from free-flowing conditions to capacity—aligning infrastructure investments and policy strategies aimed at optimizing traffic efficiency. Furthermore, the calibration methodology and validation framework outlined in the research serve as a replicable approach for evaluating different intersection solutions, supporting data-driven decision-making, and guiding the development of adaptable, future-proof road infrastructure aligned with smart mobility objectives. Acknowledging current limitations due to the scarcity of empirical CAV data, the study highlights the necessity of ongoing research, pilot projects, and adaptive infrastructure strategies to enable efficient traffic management in an era increasingly dominated by autonomous mobility.

5. Conclusions

This paper presents a validation-driven approach within a microsimulation environment to compare various intersection solutions and analyze how traffic settings involving connected and automated mobility can be channeled into road intersection design, thereby promoting the sustainable integration of smart vehicles into current and future road infrastructure. Focusing on comparing a signalized intersection with a two-lane roundabout and an innovative knee-turbo roundabout design under varying CAV-MERs and guided by the key questions posed in Section 1, this approach addresses practical challenges in the transition to smart mobility. An additional contribution is the proposal of a turbo roundabout design variant, tailored to accommodate the specific traffic and surrounding features of the case study context. Thus, the research bridges emerging CAV technologies and road engineering, contributing to demonstrating how intersection design can be optimized for mixed traffic environments towards fully autonomous mobility. It establishes a detailed microsimulation setup, sensitivity analysis, and calibration against RCFs, supported by field data from a signalized intersection at Opole, Poland. The proposed framework for calibration and cross-comparison aims to provide a methodological contribution, especially for practitioners assessing the feasibility of future intersection models before detailed design work begins, which requires further technical elaboration.

Results reveal that CAV operations can be influenced by intersection layout and CAV-MERs: signalized intersections tend to outperform roundabouts in capacity at high CAV levels, whereas roundabouts more effectively reduce delays under undersaturated traffic conditions. These insights offer valuable guidance for planners and road engineers, assisting in design decisions and providing a prospective outlook on scenarios leading to fully smart navigation. This aligns with evolving road engineering needs and underscores the role of ITS in this transition [1,2,34].

While the findings lay the groundwork for future studies across different scales and urban contexts, they are limited by the hypotheses, assumptions, and core concepts underpinning the simulation environment. Nonetheless, the literature within the smart cities context supports results aligned with this study's objectives (e.g., [11,19,20,24,25]). Given the scarcity of empirical data on high communication-level smart vehicles, assumptions about CAV behavior remain vital for evaluating operational potential [1,20]. Despite current data limitations, the study emphasizes the importance of ongoing research, pilot projects, and adaptive infrastructure strategies to support efficient traffic management in the era of autonomous mobility. However, this research sets a precedent for systematically assessing

a broader range of design alternatives, including advanced technological solutions like different traffic control strategies and adaptive signaling, to evaluate sustainability across design options. The approach can facilitate the assessment of CAV efficiency relative to road geometry and driving behavior shifts, as well as develop expertise in comparing diverse intersection proposals involving CAVs. Ultimately, the findings offer valuable insights into the operational benefits of smart mobility in relation to road geometry, while the methodology provides transportation planners and engineers with alternative tools to evaluate intersection designs aligned with the gains expected from smart mobility.

To generalize results and accurately model transition scenarios, future research should extend investigations of CAV driving behavior on a wider scale. Collecting real-world behavioral data will enhance robustness, applicability, and precision. Additionally, validation should go beyond the entrance mechanism analogy for isolated intersections, encompassing other control modes and traffic demands across diverse urban contexts. This would support broader generalization across road networks and traffic flow structures.

Further, future studies should consider incorporating greater behavioral variability of CAVs—not only at fixed signalized intersections and roundabouts but also at actuated intersections—to reflect operational realities more accurately. Achieving full integration of CAVs into road design assessment practices will require collaborative efforts among stakeholders involved in smart mobility development. Future directions include expanding empirical research on CAV behavior and creating frameworks for implementing innovative intersection designs that incorporate smart mobility advancements throughout their lifecycle, ultimately fostering sustainable transportation practices.

Author Contributions: Conceptualization, M.L.T., N.Z., E.M. and A.G.; methodology, M.L.T., N.Z., E.M. and A.G.; software, M.L.T.; validation, M.L.T.; formal analysis, M.L.T. and E.M.; investigation, M.L.T., E.M. and A.G.; resources, M.L.T., E.M. and A.G.; data curation, M.L.T., N.Z., E.M. and A.G.; writing—original draft preparation, E.M. and A.G.; writing—review and editing M.L.T., N.Z., E.M. and A.G.; visualization, M.L.T., E.M. and A.G.; supervision, E.M. and A.G.; project administration, M.L.T., E.M. and A.G.; funding acquisition M.L.T., E.M. and A.G. All authors have read and agreed to the published version of the manuscript.

Funding: This research received no external funding.

Data Availability Statement: The data are made available by the corresponding authors upon kind request.

Acknowledgments: This publication is supported by the Rector's Professor Grant, Silesian University of Technology, Poland, grant number 12/040/SDU/10-07-01.

Conflicts of Interest: The authors declare no conflicts of interest.

Abbreviations

The following abbreviations are used in this manuscript:

ITS	Intelligent Transport Systems
CAVs	Connected and Automated Vehicles
VHDs	Vehicles with Human Drivers
MERs	Market Entry Rates
CAV-MERs	Market Entry Rates for CAVs
RCFs	Reference Capacity Functions
CACC	Cooperative Adaptive Cruise Control
V2V	vehicle-to-vehicle
L	exclusive left-turn lane
R&T	shared right-turn and through lane
LEL	left entry lane

REL	right entry lane
N-E	north-east
E-S	east-south
S-W	south-west
W-N	west-north
CACC-CAVs	Connected and Automated Vehicles with the Cooperative Adaptive Cruise Control system
GEH	Geoffrey index
s.e.	standard error
RMSNE	root mean squared normalized error

References

1. Pompigna, A.; Mauro, R. Smart Roads: A State of the Art of Highways Innovations in the Smart Age. *Eng. Sci. Technol. Int. J.* **2022**, *25*, 100986. [CrossRef]
2. Makridis, M.; Mattas, K.; Mogno, C.; Ciuffo, B.; Fontaras, G. The impact of automation and connectivity on traffic flow and CO_2 emissions: A detailed microsimulation study. *Atmos. Environ.* **2020**, *226*, 117399. [CrossRef]
3. Matin, A.; Dia, H. Impacts of connected and automated vehicles on road safety and efficiency: A systematic literature review. *IEEE Trans. Intell. Transp. Syst.* **2023**, *24*, 2705–2736. [CrossRef]
4. SAE International. SAE J3016 Automated-Driving Graphic. Available online: https://www.sae.org/news/2019/01/sae-updates-j3016-automated-driving-graphic (accessed on 30 March 2025).
5. Malik, S.; Khan, M.A.; El-Sayed, H.; Khan, M.J. Should Autonomous Vehicles Collaborate in a Complex Urban Environment or Not? *Smart Cities* **2023**, *6*, 2447–2483. [CrossRef]
6. Sadaf, M.; Iqbal, Z.; Javed, A.R.; Saba, I.; Krichen, M.; Majeed, S.; Raza, A. Connected and Automated Vehicles: Infrastructure, Applications, Security, Critical Challenges, and Future Aspects. *Technologies* **2023**, *11*, 117. [CrossRef]
7. Ni, D. *Signalized Intersections*, 1st ed.; Springer: Cham, Swizerland, 2020; p. XV, 335. [CrossRef]
8. Tahiri, M.A.; Rachid, A.; Boudmane, B.; Mortabit, I.; Laaroussi, S. Toward Cooperative Adaptive Cruise Control: A Mini-review. In Proceedings of the International Conference on Circuit, Systems and Communication (ICCSC), Fes, Morocco, 28–29 June 2024; pp. 1–6. [CrossRef]
9. Xu, L.; Ma, J.; Zhang, S.; Wang, Y. Car following models for alleviating the degeneration of CACC function of CAVs in weak platoon intensity. *Transp. Lett.* **2023**, *16*, 599–611. [CrossRef]
10. Karbasi, A.; O'Hern, S. Investigating the Impact of Connected and Automated Vehicles on Signalized and Unsignalized Intersections Safety in Mixed Traffic. *Future Transp.* **2022**, *2*, 24–40. [CrossRef]
11. Tumminello, M.L.; Macioszek, E.; Granà, A.; Giuffrè, T. Simulation-Based Analysis of "What-If" Scenarios with Connected and Automated Vehicles Navigating Roundabouts. *Sensors* **2022**, *22*, 6670. [CrossRef]
12. National Academies of Sciences, Engineering, and Medicine. *Guide for Roundabouts*; The National Academies Press: Washington, DC, USA, 2023. [CrossRef]
13. National Academies of Sciences, Engineering, and Medicine. *Highway Capacity Manual: A Guide for Multimodal Mobility Analysis*, 7th ed.; The National Academies Press: Washington, DC, USA, 2022. [CrossRef]
14. Fortuijn, L.G. Turbo roundabouts: Design principles and safety performance. *Transp. Res. Rec.* **2009**, *2096*, 16–24. [CrossRef]
15. Tollazzi, T. Alternative Types of Roundabouts at Development Phases. In *Alternative Types of Roundabouts. Springer Tracts on Transportation and Traffic*, 1st ed.; Springer: Cham, Swizerland, 2015; Volume 6, pp. 157–169. [CrossRef]
16. Barceló, J. *Fundamentals of Traffic Simulation*, 1st ed.; Springer: New York, NY, USA, 2010; p. 442. [CrossRef]
17. Aimsun Next. *Version 20 Dynamic Simulator User Manual*; TSS-Transport Simulation Systems: Barcelona, Spain, 2020.
18. Ahmed, H.U.; Ahmad, S.; Yang, X.; Lu, P.; Huang, Y. Safety and Mobility Evaluation of Cumulative-Anticipative Car-Following Model for Connected Autonomous Vehicles. *Smart Cities* **2024**, *7*, 518–540. [CrossRef]
19. Song, L.; Fan, W.; Liu, P. Exploring the effects of connected and automated vehicles at fixed and actuated signalized intersections with different market penetration rates. *Transp. Plan. Technol.* **2021**, *44*, 577–593. [CrossRef]
20. Hajbabaie, A.; Tajalli, M.; Bardaka, E. Effects of connectivity and automation on saturation headway and capacity at signalized intersections. *Transp. Res. Rec.* **2023**, *2678*, 31–46. [CrossRef]
21. Jiang, Y.; Cong, H.; Chen, H.; Yao, Z. Safety evaluation for mixed traffic flow of CAVs with different automation and connection levels. *Expert. Syst. Appl.* **2025**, *261*, 125561. [CrossRef]
22. Tong, H.; Xu, C.; Ai, Q.; Ren, W.; Wang, C.; Peng, C.; Jiao, Y. Developing a jam-absorption strategy for mixed traffic flow at signalized intersections using deep reinforcement learning. *Transp. Lett.* **2024**, 1–12. [CrossRef]

23. Li, D.; Zhu, F.; Wu, J.; Wong, Y.D.; Chen, T. Managing mixed traffic at signalized intersections: An adaptive signal control and CAV coordination system based on deep reinforcement learning. *Expert. Syst. Appl.* **2024**, *238 Pt C*, 121959. [CrossRef]
24. Mohebifard, R.; Hajbabaie, A. Trajectory control in roundabouts with a mixed fleet of automated and human-driven vehicles. *Comput.-Aided Civ. Infrastruct. Eng.* **2022**, *37*, 1959–1977. [CrossRef]
25. Martin-Gasulla, M.; Elefteriadou, L. Traffic management with autonomous and connected vehicles at single-lane roundabouts. *Transp. Res. C Emerg. Technol.* **2021**, *125*, 102964. [CrossRef]
26. Wu, Y.; Zhu, F. Junction management for connected and automated vehicles: Intersection or roundabout? *Sustainability* **2021**, *13*, 9482. [CrossRef]
27. Turbo Roundabouts Informational Primer. FHWA Safety Program. In *Federal Highway Administration*; U.S. Department of Transportation: Washington, DC, USA, 2022. Available online: https://highways.dot.gov/sites/fhwa.dot.gov/files/2022-06/fhwasa20019_0.pdf (accessed on 20 March 2025).
28. Gkyrtis, K.; Kokkalis, A. An overview of the efficiency of roundabouts: Design aspects and contribution toward safer vehicle movement. *Vehicles* **2024**, *6*, 433–449. [CrossRef]
29. Ministry of Infrastructure. Guidelines for the design of road intersections. In *Part 3: Roundabouts*; WR-D-31-3; Ministry of Infrastructure: Warsaw, Poland, 2022.
30. Garg, M.; Bouroche, M. Can Connected Autonomous Vehicles Improve Mixed Traffic Safety Without Compromising Efficiency in Realistic Scenarios? *IEEE Trans. Intell. Transp. Syst.* **2023**, *24*, 6674–6689. [CrossRef]
31. Gipps, P.G. A Behavioural Car-Following Model for Computer Simulation. *Transp. Res. Part B* **1981**, *15*, 105–111. [CrossRef]
32. Sadid, H.; Antoniou, C. Modelling and simulation of (connected) autonomous vehicles longitudinal driving behavior: A state-of-the-art. *IET Intell. Transp. Syst.* **2023**, *17*, 1050–1070. [CrossRef]
33. Mauro, R.; Branco, F. Comparative analysis of compact multilane roundabouts and turbo-roundabouts. *J. Transp. Eng.* **2010**, *136*, 316–322. [CrossRef]
34. Emami, A.; Sarvi, M.; Asadi Bagloee, S. A review of the critical elements and development of real-world connected vehicle testbeds around the world. *Transp. Lett.* **2020**, *14*, 49–74. [CrossRef]
35. PTV Planung Transport Verkehr AG. *PTV VISSIM User Manual*; PTV Planung Transport Verkehr AG: Karlsruhe, Germany, 2017.